J|A|C|S
ARTICLES
Published on Web 02/03/2006

Theoretical Investigations on Chalcogen−Chalcogen Interactions: What Makes These Nonbonded Interactions Bonding?

Christian Bleiholder,[†,‡] Daniel B. Werz,[†,§] Horst Köppel,[⊥] and Rolf Gleiter*[,†]

Contribution from the Organisch-Chemisches Institut der Universität Heidelberg, Im Neuenheimer Feld 270, D-69120 Heidelberg, Germany, Deutsches Krebsforschungszentrum (DKFZ), Im Neuenheimer Feld 280, D-69120 Heidelberg, Germany, Laboratorium für Organische Chemie, Wolfgang-Pauli-Strasse 10, Swiss Federal Institute of Technology Zürich, ETH-Hönggerberg, HCI F 306, CH-8093 Zürich, Switzerland, and Physikalisch-Chemisches Institut der Universität Heidelberg, Im Neuenheimer Feld 229, D-69120 Heidelberg, Germany

Received October 6, 2005; E-mail: rolf.gleiter@oci.uni-heidelberg.de

Abstract: To understand the intermolecular interactions between chalcogen centers (O, S, Se, Te), quantum chemical calculations on pairs of model systems were carried out. For the oxygen derivatives, one of the components of the supermolecules consists of dimethyl ether, while the second component is either dimethyl ether (**1**) or ethynyl methyl ether (**2**) or methyl cyanate (**3**). The model calculations were also extended to the sulfur (**4**−**6**), selenium (**7**−**9**), and tellurium congeners (**10**−**12**). The MP2/SDB-cc-pVTZ, 6-311G* level of theory was used to derive the geometrical parameters and the global energies of the model systems. A detailed analysis based on symmetry adapted perturbation theory (SAPT) reveals that induction and dispersion forces contribute to the bonding in each case. For **1**−**3** the electrostatic energy also contributes to the intermolecular bonding, but not for **4**−**12**. The NBO analysis reveals that the interaction in the dimers **1**−**3** is mainly due to weak hydrogen bonding between methyl groups and chalcogen centers. Similar hydrogen bonding is also found in the case of **4** and to a lesser extent in **5** and **7**. For the aggregates with heavier centers the chalcogen−chalcogen interaction dominates, and hydrogen bonding only plays a minor role. Electron-withdrawing groups on the chalcogen centers increase the interaction energy and reduce the intermolecular distance dramatically. The one-electron picture of an interaction between the lone pair of the donor and the chalcogen carbon σ^* orbital allows a qualitatively correct reproduction of the observed trend.

Introduction

Supramolecular chemistry is based on noncovalent bonding interactions.[1−3] This term includes a large range of attractive and repulsive forces.[2,3] The most important ones are hydrogen bonding, ion−ion interactions, ion−dipole interactions, $\pi-\pi$ interactions, dipole−dipole interactions, and van der Waals forces. These forces are responsible for the self-assembly of large molecules, crystal packing, and biological pattern recognition, to name just a few examples.

The most attractive supramolecular units resulting from noncovalent bonding interactions are helices and tubes. Examples for such structures are found in amylose which consists of 1,4-glycosidic linked α-D-glucose units.[4] In transmembrane channels, such as the potassium channel[5] or the maltoporin channel,[6] bundles of helical proteins form a hollow tube. Another way of generating tubes is the stacking of cyclic units. This has been exemplified by cyclic peptides,[7] by dipeptides as building blocks,[8] and by cyclodextrins.[9] However, shape-persistent macrocycles with phenol units as aromatic building blocks also form stacks with tubular structures.[10] Common to all these examples are hydrogen bonds as directional weak forces.

A further directional force which leads to self-assembly of molecules are short interactions between halogen centers[11] and

[†] Organisch-Chemisches Institut der Universität Heidelberg.
[‡] Deutsches Krebsforschungszentrum (DKFZ).
[§] Swiss Federal Institute of Technology Zürich (ETH Zürich).
[⊥] Physikalisch-Chemisches Institut der Universität Heidelberg.

(1) Lehn, J.-M. *Supramolecular Chemistry: Concepts and Perspectives*; VCH: Weinheim, 1995.
(2) Steed, J. W.; Atwood, J. L. *Supramolecular Chemistry*; John Wiley & Sons: Chichester, 2000.
(3) Schneider, H. J.; Yatsimirsky, A. *Principles and Methods in Supramolecular Chemistry*; John Wiley & Sons: Chichester, 2000.
(4) Bishop, R.; Dance, I. G. *Top. Curr. Chem.* **1988**, *149*, 137−188 and references therein.
(5) Doyle, D. A.; Cabral, J. M.; Pfuetzner, R. A.; Kuo, A.; Gulbis, J. M.; Cohen, S. L.; Chait, B. T.; McKinnon, R. *Science* **1998**, *280*, 69−77.
(6) Schirmer, T.; Keller, T. A.; Wang, Y.-F.; Rosenbusch, J. P. *Science* **1995**, *267*, 512−514.
(7) Bong, D. T.; Clark, T. D.; Granja, J. R.; Ghadiri, M. R. *Angew. Chem.* **2001**, *113*, 1016−1041; *Angew. Chem., Int. Ed.* **2001**, *40*, 988−1011 and references therein.
(8) Görbitz, C. H. *Chem. Eur. J.* **2001**, *7*, 5153−5159.
(9) Saenger, W. In *Inclusion Compounds*; Atwood, J. L., Davies, J. E., MacNicol, D. D., Eds.; Academic Press: London, 1984; Vol. 2, pp 231−259.
(10) (a) Venkataraman, D.; Lee, S.; Zhang, J.; Moore, J. S. *Nature* **1994**, *371*, 591−593. (b) Henze, O.; Lentz, D.; Schlüter, A. D. *Chem. Eur. J.* **2000**, *6*, 2362−2367. (c) Höger, S.; Morrison, D. L.; Enkelmann, V. *J. Am. Chem. Soc.* **2002**, *124*, 6734−6736.

10.1021/ja056827g CCC: $33.50

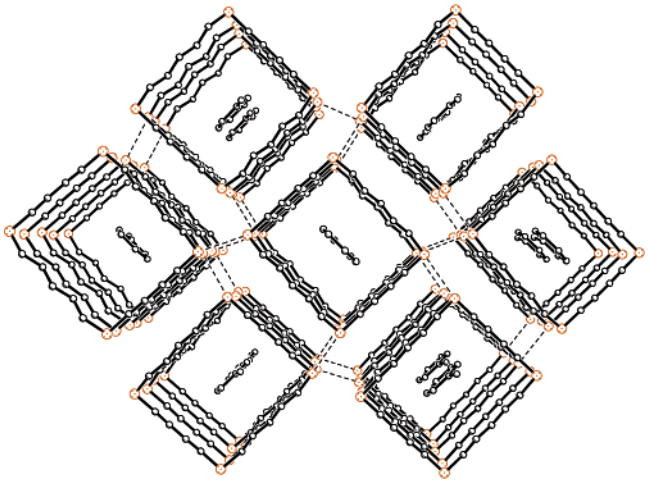

Figure 1. Columnar structure of 1,6,12,17-tetrathiacyclodocosa-2,4,13,15-tetrayne in the solid state with included toluene guest molecules. H atoms are omitted for the sake of clarity.

between chalcogen centers.[12] These forces are ascribed as van der Waals forces which usually do not show much directionality. As a result two- and three-dimensional networks are obtained,[13] but no helical or tubular structures. We have been able to observe columnar structures and even nanotubes in the solid state using cyclic systems which contain chalcogen atoms (Figure 1).[14]

A large variety of cyclic as well as noncyclic compounds have been successfully synthesized. In the resulting crystal structures the distances between the chalcogen centers of neighboring molecules are smaller than the sum of the van der Waals radii of the respective atoms.[14]

By reducing the number of chalcogen centers in the cycles by 50%, we found that the tubular structures in the sulfur-containing compounds are due to weak hydrogen bonding between the C−H group and the triple bond. For the rings with Se and Te centers the chalcogen−chalcogen interactions prevail.[15] However, hydrogen bonding due to close contacts between the respective chalcogen and C−H groups is also anticipated. These contacts share structural features with the so-called improper, blue-shifted hydrogen bonds,[16,17] which are the subject of recent intense discussions.

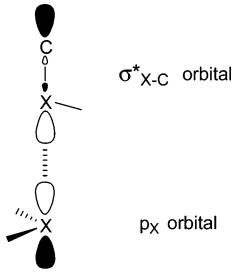

Figure 2. Directional bonding of two chalcogen centers in R−X−R′ units by np−σ* interaction.

Statistical analyses of crystal structures containing van der Waals contacts between sulfur and selenium centers (using the Cambridge Crystallographic Data Base) revealed preferred conformations. They were interpreted in terms of electrophilic−nucleophilic interactions of two chalcogen centers or as p−σ* interactions by considering the corresponding frontier orbitals (see Figure 2).[12] Other authors have named close contacts containing divalent chalcogens as "premature hypervalent bonds",[18] "secondary bonding",[19] "fractional bonding",[20] or "specific noncovalent bonding",[21] indicating uncertainty about the nature of the bonding contribution.

Contacts between divalent selenium and nitrogen, oxygen or fluorine have been intensively studied by X-ray[22] as well as NMR techniques[23,24] using cleverly designed model compounds in which both interacting centers were attached in close proximity. These investigations allowed an estimation of the strength of the selenium−nitrogen interaction between 7 and 20 kcal/mol, depending on the model system.

Quantum chemical calculations on noncovalent interactions between two molecules with closed shell centers of period 3 and higher have been carried out using various methods.[25] In the early days of applied quantum chemistry semiempirical methods[26] were used, followed by HF-SCF[18] and DFT[27] procedures. These calculations helped at most to understand these interactions qualitatively. Very recently the nature of the supramolecular association of 1,2,5-chalcogenadiazoles was investigated by applying relativistic density functional theory.[28] It was found that the main contributions stem from the interaction between the nitrogen lone pair and a chalcogen−nitrogen p−σ* orbital as well as electrostatic interactions. Correlation effects seem to play no major role.

The availability of fast correlated ab initio methods and our long-standing interest in noncovalent chalcogen−chalcogen interactions,[29] especially in the self-assembly of rings,[13,14] led us to investigate systematically the strength, the directional preferences, and the quantum mechanical nature of noncovalent

(11) Pedireddi, V. R.; Reddy, D. S.; Goud, B. S.; Craig, D. C.; Rae, A. D.; Desiraju, G. R. *J. Chem. Soc., Perkin Trans. 2* **1994**, 2353−2360.
(12) (a) Rosenfield, R. E.; Parthasarathy, R.; Dunitz, J. D. *J. Am. Chem. Soc.* **1977**, *99*, 4860−4862. (b) Glusker, J. P. *Top. Curr. Chem.* **1998**, *198*, 1−56. (c) Guru Row, T. N.; Parthasarathy, R. *J. Am. Chem. Soc.* **1981**, *103*, 477−479. (d) Ramasubbu, N.; Parthasarathy, R. *Phosphorus Sulfur* **1987**, *31*, 221−229.
(13) Williams, J. M.; Ferraro, J. R.; Thorn, R. J.; Carlson, K. D.; Geiser, U.; Wang, H. H.; Kini, A. M.; Whangbo, M.-H. *Organic Superconductors*; Prentice Hall: Englewood Cliffs, NJ, 1992.
(14) (a) Werz, D. B.; Staeb, T. H.; Benisch, C.; Rausch, B. J.; Rominger, F.; Gleiter, R. *Org. Lett.* **2002**, *4*, 339−342. (b) Werz, D. B.; Gleiter, R.; Rominger, F. *J. Am. Chem. Soc.* **2002**, *124*, 10638−10639. (c) Gleiter, R.; Werz, D. B.; Rausch, B. J. *Chem. Eur. J.* **2003**, *9*, 2676−2683. (d) Werz, D. B.; Gleiter, R.; Rominger, F. *J. Org. Chem.* **2004**, *69*, 2945−2952. (e) Gleiter, R.; Werz, D. B. *Chem. Lett.* **2005**, *34*, 126−131.
(15) Schulte, J. H.; Werz, D. B.; Rominger, F.; Gleiter, R. *Org. Biomol. Chem.* **2003**, *1*, 2788−2794.
(16) (a) Gu, Y.; Kar, T.; Scheiner, S. *J. Am. Chem. Soc.* **1999**, *121*, 9411−9422. (b) Alabugin, I. V.; Manoharan, M.; Peabody, S.; Weinhold, F. *J. Am. Chem. Soc.* **2003**, *125*, 5973−5987.
(17) (a) van der Veken, B. J.; Herrebout, W. A.; Szostak, R.; Shchepkin, D. N.; Havlas, Z.; Hobza, P. *J. Am. Chem. Soc.* **2001**, *123*, 12290−12293. (b) Delanoye, S. N.; Herrebout, W. A.; van der Veken, B. J. *J. Am. Chem. Soc.* **2002**, *124*, 7490−7498. (c) Tatamitani, Y.; Liu, B.; Shimada, J.; Ogata, T.; Ottaviani, P.; Maris, A.; Caminati, W.; Alonso, J. L. *J. Am. Chem. Soc.* **2002**, *124*, 2739−2743.
(18) Ángyán, J. G.; Poirier, R. A.; Kucsman, A.; Csizmadia, I. G. *J. Am. Chem. Soc.* **1987**, *109*, 2237−2245.
(19) (a) Alcock, N. W. *Adv. Inorg. Chem. Radiochem.* **1972**, *15*, 1−58. (b) Landrum, G. A.; Hoffmann, R. *Angew. Chem.* **1998**, *110*, 1989−1992; *Angew. Chem., Int. Ed.* **1998,** *37***,** 1887−1890.
(20) Bürgi, H. B.; Dunitz, J. D. *J. Am. Chem. Soc.* **1987**, *109*, 2924−2926.
(21) Masunov, A. E.; Zorky, P. M. *Zh. Struct. Khim.* **1992**, *33*, 105−118.
(22) Iwaoka, M.; Takemoto, S.; Okada, M.; Tomoda, S. *Bull. Chem. Soc. Jpn.* **2002**, *75*, 1611−1625.
(23) Iwaoka, M.; Tomoda, S. *J. Am. Chem. Soc.* **1996**, *118*, 8077−8084.
(24) Iwaoka, M.; Komatsu, H.; Katsuda, T.; Tomoda, S. *J. Am. Chem. Soc.* **2002**, *124*, 1902−1909.
(25) Pyykkö, P. *Chem. Rev.* **1997**, *97*, 597−636 and references therein.
(26) Boyd, D. B. *J. Phys. Chem. B* **1978**, *82*, 1407−1416.
(27) Sanz, P.; Yáñez, M.; Mó, O. *J. Phys. Chem. A* **2002**, *106*, 4661−4668.
(28) Cozzolino, A. F.; Vargas-Baca, I.; Mansour, S.; Mahmoudkhani, A. H. *J. Am. Chem. Soc.* **2005**, *127*, 3184−3190.
(29) Gleiter, R.; Gygax, R. *Top. Curr. Chem.* **1976**, *63*, 49−88.

contacts between chalcogen (O, S, Se, Te) centers. We base our conclusions on three different approaches. First, the supermolecular approach is utilized to obtain accurate interaction energies and minimum energy geometries. Perturbation theoretic calculations are performed to investigate the electronic nature of the interaction, and NBO analysis is employed in order to identify the principal interacting chemical groups. Special consideration has been paid to the mutual competition between weak hydrogen bonding and interactions between the chalcogen centers in the course of the group VI elements when going from oxygen via sulfur and selenium to tellurium.

Computational Details

Definition of Interaction Energy. Throughout this paper we use the terms "noncovalent" and "intermolecular" interactions to describe the same phenomenon: a minimum of the potential energy hypersurface (PES) in the configuration space of the Born−Oppenheimer approximation, which is observed at rather large interatomic distances and is of a different electronic nature than the so-called chemical bond. The energy connected with such an intermolecular interaction, denoted as E_{int}, is defined according to eq 1.

$$E_{int}(\vec{\mathbf{r}}, \vec{\zeta}, Q_A, Q_B) = E_{AB}(\vec{\mathbf{r}}, \vec{\zeta}, Q_A, Q_B) - E_A(Q_A) - E_B(Q_B) \quad (1)$$

This equation defines the interaction energy (E_{int}) as the difference between the energy of a supermolecule E_{AB} and the separated monomers (E_A, E_B), where the monomers are in the same internal coordinates Q_A, Q_B as in the supermolecule. The relative orientation of the monomers is described using the intermolecular vector $\vec{\mathbf{r}}$ and the orientational angles $\vec{\zeta}$. Unless otherwise noted all quantities in this work are corrected for basis set superposition effects (BSSE) using the counterpoise (CP) procedure.[27] The interaction energies will be denoted as $E^{basis}_{int,method}$.

Choice of Basis Sets and Methods. Selection of the basis set has proven to be difficult for our purposes. Several studies have revealed that at least a polarization or diffuse augmented split-valence triple-ζ basis set in combination with electron-correlation methods is needed to obtain reliable results for van der Waals type interactions.[31] Additionally, a good effective core potential (ECP) was needed, at least for tellurium-containing compounds. Hence, we have chosen the family of Dunning's correlation consistent basis sets (correlation consistent polarized valence triple-ζ, cc-pVnZ,[32] cc-pVnZ-PP,[33] SDB-cc-pVnZ[34]) for which high-quality small- and large-core ECPs have recently been derived.[51] Benchmarking was done using these basis sets combined with Pople's 6-311G family for the lighter atoms (H, C, N)[35] with and without polarization and diffuse functions in combination with a variety of electronic structure methods (HF,[36] MPn,[37] CCSD(T),[38] B3LYP[39]). In this study we varied the distance between the two chalcogen centers of four small model compounds leaving all other geometrical parameters fixed. This investigation revealed that the MP2/SDB-cc-pVTZ, 6-311G* as well as the MP3/SDB-aug-cc-pVTZ, 6-311++G** levels of theory provide a very efficient way for estimating the coupled cluster CCSD(T)/aug-cc-pVTZ-PP, 6-311++G**[33,35] interaction energies. In the course of this work, these basis sets SDB-cc-pVTZ, 6-311G*[33,35] are denoted as cc-pVTZ-ECP and SDB-aug-cc-pVTZ, 6-311++G**[33,35] as aug-cc-pVTZ-ECP. As an example, the results obtained for the interaction of TeH_2 with Te(H)CN are shown in Figure 3 (see Supporting Information (SI) for details). The Hartree−Fock (HF) level of theory[36] turned out to be insufficient for describing the interaction between two divalent chalcogens and led to supermolecule geometries with too long intermolecular distances. However, it predicts a bonding interaction between the two chalcogen centers. The B3LYP method[39] leads to quite good geometries but is incapable of recovering much of the interaction energy. This finding is very important also in the light of previous investigations. In contrast to HF and B3LYP the other three methods provide very similar results with respect to the minimum and the interaction energy (see SI for more details and information).

For the model systems shown below (Chart 1) we optimized the geometrical parameters with Gaussian03[40] using the counterpoise protocol to obtain BSSE-corrected[41] supramolecular geometries. Each geometry has been characterized as a minimum by a subsequent frequency calculation.

Special attention was paid to the flatness of a van der Waals PES. Therefore, the convergence criteria during geometry optimizations were set rather tight to reach the minima as closely as possible. Additionally,

(30) Boys, S. F.; Bernardi, F. *Mol. Phys.* **1970**, *19*, 535−539.
(31) DelBene, J. E.; Shavitt, I. *In Molecular Interactions*; Scheiner, S., Ed.; John Wiley & Sons: New York, 1997; pp 157−179.
(32) (a) Dunning, T. H., Jr.; Thom, H.; Peterson, K. A. *Encyclopedia of Computational Chemistry*; Schleyer, P. v. R., Ed.; Wiley: New York, 1998; Vol. 1, 88−115. (b) Dunning, T. H., Jr. *J. Chem. Phys.* **1989**, *90*, 1007−1023.
(33) (a) Peterson, K. A. *J. Chem. Phys.* **2003**, *119*, 11099−11112. (b) Peterson, K. A.; Figgen, D.; Goll, E.; Stoll, H.; Dolg, M. *J. Chem. Phys.* **2003**, *119*, 11113−11123. (c) Metz, B.; Schweizer, M.; Stoll, H.; Dolg, M.; Liu, W. *Theor. Chem. Acc.* **2000**, *104*, 22−28. (d) Metz, B.; Stoll, H.; Dolg, M. *J. Chem. Phys.* **2000**, *113*, 2563−2569.
(34) (a) Martin, J. M. L.; Sundermann, A. *J. Chem. Phys.* **2001**, *114*, 3408−3420. (b) Bergner, A.; Dolg, M.; Kuechle, W.; Stoll, H.; Preuss, H. *Mol. Phys.* **1993**, *80*, 1431−1441.
(35) (a) Krishnan, R.; Binkley, J. S.; Seeger, R.; Pople, J. A. *J. Chem. Phys.* **1980**, *72*, 650−654. (b) McLean, A. D.; Chandler, G. S. *J. Chem. Phys.* **1980**, *72*, 5639−5648. (c) Curtiss, L. A.; McGrath, M. P.; Blaudeau, J.-P.; Davis, N. E.; Binning, R. C., Jr.; Radom, L. *J. Chem. Phys.* **1995**, *103*, 6104−6113. (d) Clark, T.; Chandrasekhar, J.; Spitznagel, G. W.; Schleyer, P. v. R. *J. Comput. Chem.* **1983**, *4*, 294−301.
(36) (a) Hartree, D. R. *The Calculations of Atomic Structures*; Wiley: New York, 1957. (b) Roothaan, C. C. J. *Rev. Mod. Phys.* **1960**, *32*, 179−185. (c) Huzinaga, S. *Phys. Rev.* **1960**, *120*, 866−871, *Phys. Rev.* **1961**, *122*, 131−138. (d) Veszprémi, T.; Fehér, M. *Quantum Chemistry: Fundamentals to Applications*; Kluwer - Academic Plenum Publishing: Dordrecht, 1999.
(37) (a) Møller, C.; Plesset, M. S. *Phys. Rev.* **1934**, *46*, 618−622. (b) Pople, J. A.; Seeger, R.; Krishnan, R. *Int. J. Quantum Chem. Symp.* **1977**, *11*, 149−161. (c) Pople, J. A.; Binkley, J. S.; Seeger, R. *Int. J. Quantum Chem. Symp.* **1976**, *10*, 1−17.
(38) (a) Pople, J. A.; Krishnan, R.; Schlegel, H. B.; Binkley, J. S. *Int. J. Quantum Chem.* **1978**, *14*, 545−560. (b) Bartlett, R. J.; Purvis, G. D. *Int. J. Quantum Chem.* **1978**, *14*, 516−531. (c) Cizek, *J. Adv. Chem. Phys.* **1969**, *14*, 35−45. (d) Purvis, G. D.; Bartlett, R. J. *J. Chem. Phys.* **1982**, *76*, 1910−1918. (e) Scuseria, G. E.; Schaefer, H. F., III. *J. Chem. Phys.* **1988**, *89*, 7382−7387. (f) Scuseria, G. E.; Schaefer, H. F., III. *J. Chem. Phys.* **1989**, *90*, 3700−3703. (g) Pople, J. A.; Head-Gordon, M.; Raghavachari, K. *J. Chem. Phys.* **1987**, *87*, 5968−5975.
(39) (a) Lee, C.; Yang, W.; Parr, R. G. *Phys. Rev. B.* **1988**, *37*, 785−789. (b) Miehlich, B.; Savin, A.; Stoll, H.; Preuss, H. *Chem. Phys. Lett.* **1989**, *157*, 200−206. (c) Becke, A. D. *J. Chem. Phys.* **1993**, *98*, 5648−5652.
(40) Pople J. A.; et al. *Gaussian03*, Revision B.03; Gaussian, Inc.: Wallingford CT, 2004.
(41) (a) van Duijneveldt, F. B.; van Duijneveldt-van de Rijdt, J. G. C. M.; van Lenthe, J. H. *Chem. Rev.* **1994**, *94*, 1873−1885. (b) Paizs, B.; Suhai, S. *J. Comput. Chem.* **1998**, *19*, 575−584. (c) Salvador, P.; Paizs, B.; Duran, M.; Suhai, S. *J. Comput. Chem.* **2001**, *22*, 765−786.
(42) (a) Carpenter, J. E.; Weinhold, F. *J. Mol. Struct. (THEOCHEM)* **1988**, *46*, 41−62. (b) Foster, J. P.; Weinhold, F. *J. Am. Chem. Soc.* **1980**, *102*, 7211−7218.
(43) *SAPT2002*: An Ab Initio Program for Many-Body Symmetry-Adapted Perturbation Theory Calculations of Intermolecular Interaction Energies; Bukowski, R. et al. University of Delaware and University of Warsaw, 2002.
(44) Saunders, V. R.; Guest, M. F. *ATMOL Program Package*; SERC Daresbury Laboratory: Daresbury, UK.
(45) Bleiholder, C.; Werz, D. B.; Köppel, H.; Gleiter, R. To be published.
(46) Pauling, L. *The Nature of the Chemical Bond*, 4th ed.; Cornell University Press: Ithaca, NY, 1973.
(47) Cradock, S.; Whiteford, R. A. *J. Chem. Soc., Faraday Trans. II* **1972**, *68*, 281−288.
(48) Kimma, K.; Katsumata, S.; Achiba, Y.; Yamazaki, T.; Iwata, S. *Handbook of the He(I) Photoelectron Spectra of Fundamental Organic Molecules*; Japan Scientific Societies Press: Tokyo, 1981 and references therein.
(49) Tarakeshwar, P.; Kim, S. K. *J. Mol. Struct.* **2002**, *615*, 227−238.
(50) Metrangolo, P.; Resnati, G. *Chem. Eur. J.* **2001**, *7*, 2511−2519.
(51) Basis sets were partly obtained from the Extensible Computational Chemistry Environment Basis Set Database, Version 02/25/04, as developed and distributed by the Molecular Science Computing Facility, Environmental and Molecular Sciences Laboratory which is part of the Pacific Northwest Laboratory, P.O. Box 999, Richland, WA 99352, U.S.A., and funded by the U.S. Department of Energy. The Pacific Northwest Laboratory is a multiprogram laboratory operated by Battelle Memorial Institute for the U.S. Department of Energy under contract DE-AC06-76RLO 1830. Contact Karen Schuchardt for further information.

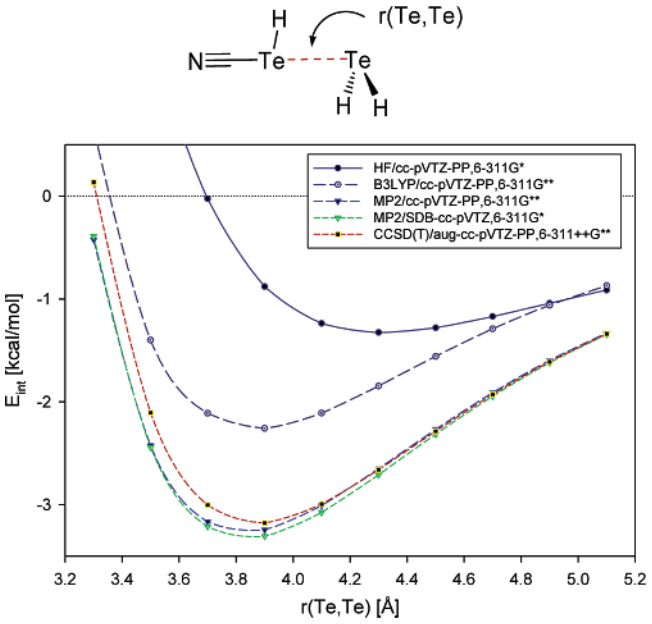

Figure 3. Potential energy curves of $H_2Te\cdots Te(H)CN$ as derived by different methods and basis sets.

Chart 1. Dimeric Model Systems **1**−**12**

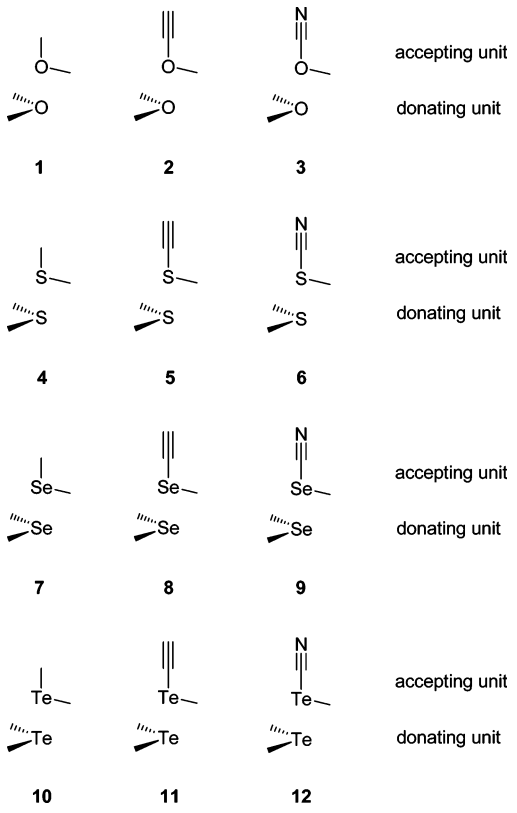

force constants were recalculated every five to ten steps. Perturbation theoretic interaction energy corrections were computed using SAPT2002.[43] For these calculations, Atmol1024[44] was used as the necessary SCF front end. These calculations have been performed on the dimer's optimized geometries using the 6-311G** basis set, since no ECPs could be applied. For this reason, SAPT calculations were not performed for the tellurium-containing systems. The energy corrections calculated by the SAPT program have been summed up to give the electrostatic, induction, dispersion as well as the exchange-correlation contributions according to eqs 3−6 below.

Table 1. Calculated energies $E_{int,MP2}^{cc-pVZ-ECP}$ [kcal/mol] and Te···Te Distances $r(X_1,X_2)$ [Å] for **10** in C_s and C_1 Symmetry

system	$E_{int,MP2}^{cc-pVTZ,ECP}$ [a]	$r(X_1,X_2)$ [a]
10 (C_s)	−3.40	3.97
10 (C_1)	−2.85	3.89

[a] Corrected for BSSE.

Natural bond orbital (NBO) analyses[42] have been employed to estimate the relative amount of hydrogen bonding compared to chalcogen−chalcogen interaction. Toward this end, NBO analyses have been performed on the dimer's optimized geometries using the HF/aug-cc-pVTZ-ECP density. Each intermonomer NBO interaction term was interpreted in terms of hydrogen-bonding or chalcogen−chalcogen interaction, depending on the atoms the NBO was placed on. Finally, they were summed up to estimate the strength of the hydrogen-bonding and chalcogen−chalcogen interactions, respectively. (See SI for a detailed description of the summation algorithm.) Charge transfer between the two molecular units was also obtained from NBO analysis. Because the charge q_i for each isolated unit is zero and $q_1 = -q_2$, the net charge transfer from molecular unit 2 to unit 1 is given by the charge of molecular unit 1.

Results and Discussion

Model Systems. As is evident from our studies of tubular aggregates (e.g., Figure 1), the contact of two different molecules in the solid state can be represented by a simple dimer. This dimer consists of two monomers, each representing one of the molecules in contact.

For a systematic discussion of the particular influences of the chalcogen atom ($\mathbf{X}_{1,2}$ = O, S, Se or Te) and of the substituents **Z** connected to the chalcogen atom we chose the model systems shown in Chart 1. As donor unit we used $H_3C-X_1-CH_3$ (X_1 = O, S, Se, Te). The accepting unit was varied from H_3C-X_2-Z (X_2 = O, S, Se, Te), with the substituent Z varied from Z = CH_3 to C_2H and CN. In particular, this substitution pattern allows an examination of the molecular orbital (MO) hypothesis depicted in Figure 2.

We concentrate in this paper on homoatomic examples ($X_1 = X_2$), which are the most extensively characterized systems by experimental means.[12] The results for heteroatomic ($X_1 \neq X_2$) interactions would exceed the scope of this paper and will be published in a forthcoming one.[45]

Optimized Geometries and Supermolecular Interaction Energies. For the model system **10** we scrutinized the PES by varying the $X_1\cdots X_2$ distance and ω. The global minimum found is of C_s-like geometry, in which the 5p orbital of the lower Te_1 center is aligned with the Te_2-CH_3 bond. However, the second CH_3 group connected to the upper Te_2 atom is slightly rotated around the Te_1-Te_2 axis, such that a true C_s-symmetric structure is not maintained. In the local minimum (C_1) such an alignment is avoided due to steric crowding between the CH_3 groups. For both conformers the distances between the chalcogen centers and the interaction energies are listed in Table 1.

For the model systems **1**−**12** we performed full geometry optimizations, i.e. in all internal parameters Q_i, $r(X_1,X_2)$, and ω_i. The parameters $r(X_1,X_2)$, and ω_i are defined in Figure 4. In Table 2 we list the calculated interaction energies for **1**−**12** at the equilibrium distances and the angles ω_i given. It can be seen that the calculated equilibrium distance $r(X_1,X_2)$ is much larger than the sum of the van der Waals radii (2.8 Å)[46] for compounds **1**−**3** only. For all other compounds **4**−**12** the calculated distance

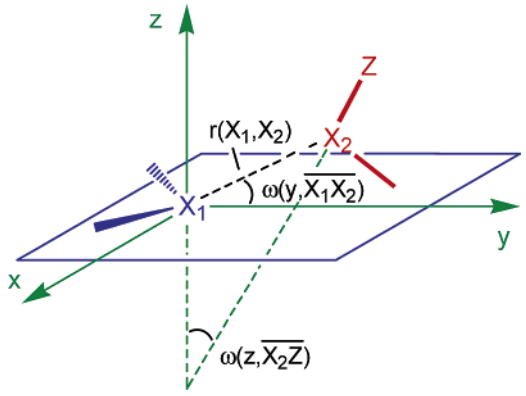

Figure 4. Definition of the three most important parameters, the distance $r(X_1,X_2)$ and the orientational angles $\omega(y,\overline{X_1X_2})$ and $\omega(z,\overline{X_1X_2})$ which have been used to characterize the optimized geometries of the model systems **1**−**12** in Table 2.

Table 2. Calculated Interaction Energies $E_{int,MP2}^{cc-pVTZ,ECP}$ [kcal/mol], Intermolecular Equilibrium Distance $r(X_1,X_2)$ [Å], Orientational Angles $\omega(y,\overline{X_1X_2})$, $\omega(z,\overline{X_2Z})$ [deg] of **1**−**12** and Change $\Delta\tilde{\nu}(X_2-Z)$ [cm^{-1}] in the Stretching Vibration of the X_2-Z Bond Due to the Aggregation

model system	$E_{int,MP2}^{cc-pVTZ,ECP}$ [a,b]	$r(X_1,X_2)$[a,b]	$\omega(y,\overline{X_1X_2})$[a,b]	$\omega(z,\overline{X_2Z})$[a,b]	$\Delta\tilde{\nu}(X_2-Z)$
1	−2.15	3.68	113.8	29.0	4.6
2	−2.58	3.52	103.1	21.2	−4.8
3	−2.95	3.43	94.2	12.8	−4.8
4	−2.79	4.03	113.9	19.7	−1.5
5	−3.23	3.63	102.0	16.8	−2.7
6	−3.85	3.38	97.8	13.7	−6.6
7	−2.82	3.91	108.1	18.0	−1.6
8	−3.66	3.63	100.0	15.3	−9.6
9	−4.62	3.50	96.9	10.7	−16.5
10	−3.40	3.97	105.7	17.9	−3.4
11	−4.64	3.76	100.5	13.7	−17.0
12	−6.18	3.61	96.9	8.8	−29.0

[a] For the definition of the parameters see Figure 4. [b] Corrected for BSSE.

$r(X_1,X_2)$ is only slightly larger (**4**) or smaller (**5**−**12**) than the sum of the van der Waals radii of S (3.7 Å),[46] Se (4.0 Å)[46] and Te (4.4 Å).[46] Most notably, the sum of the van der Waals radii of **12** is penetrated by 0.8 Å.

Changing the substituent Z from a CH_3 group to C_2H and CN decreases the distance by 0.3 to 0.6 Å. Although this decrease slightly depends on the chalcogen element, we observe a major influence of the electron-withdrawing nature of substituent Z. As anticipated from our definitions shown in Figure 4 the angle $\omega(y,\overline{X_1X_2})$ is found to be approximately 90° in all cases. We notice deviations from this arrangement depending on the substituent Z in such a way that the angle is increased with less electron-withdrawing character of Z (e.g. $\omega(CH_3) > \omega(C_2H) > \omega(CN)$). An analogous trend is observed for $\omega(z,\overline{X_2Z})$. Here, the angle also decreases with increasing electron-withdrawing character of Z. These findings can be rationalized by the MO hypothesis (Figure 2), which indicates the major bonding contribution stemming from a p−σ* orbital type interaction. Clearly, the intermonomeric distances decrease with increased bonding between the monomers. The ideal geometrical arrangement for this p−σ* type interaction takes places at $\omega(z,\overline{X_2Z}) \approx 0°$ and $\omega(y,\overline{X_1X_2}) \approx 90°$. Because in addition to this p−σ* type interaction, other forces also influence the aggregate's structure, the resulting dimers' geometries are to some extent distorted from this idealized p−σ* geometry. Hydrogen bonding between a chalcogen atom and a C−H group

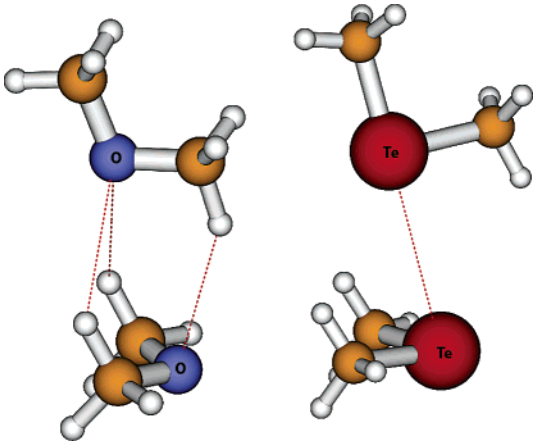

Figure 5. Minimum geometries of the dimers **1** (left) and **10** (right).

favors larger values for angles $\omega(z,\overline{X_2Z})$ and $\omega(y,\overline{X_1X_2})$. Therefore, their decrease in each family of S, Se, and Te is attributed to an increased dominance of p−σ* type interaction together with an increased electron-withdrawing character of Z. Although an analogous trend is seen for the structures of **1**−**3** as well as for **4**−**12**, the high compactness of oxygen renders them distinct from the latter. Here, steric repulsion between the methyl groups (van der Waals radius of CH_3 = 2.0 Å)[46] must be taken into account for **1**−**3**. This prevents the oxygen atoms from approaching each other any closer than the sum of their van der Waals radii. As a result, a similar geometry as expected from a p−σ* type interaction emerges. In Figure 5 we show the structures of minimum energy obtained for **1** and **10**.

In **1** we encounter three C−H···O hydrogen bonds as described in the literature.[16,17] In contrast, the geometry of **10** is determined by a p−σ* interaction between the 5p lone pair of dimethyl telluride and the σ* orbital localized at the Te−C(sp) bond. Considering the energetic data presented in Table 2, similar trends are observed for the interaction energy $E_{int,MP2}^{cc-pVTZ-ECP}$. Here, we note an increase in the interaction energy by 0.79 (O), 1.07 (S), 1.80 (Se), and 2.78 (Te) kcal/mol when changing Z from CH_3 via C_2H to CN. Although the substituent Z again has the major influence on the interaction energy, the increase in $E_{int,MP2}^{cc-pVTZ-ECP}$ is strongly affected by the element number of the chalcogens involved. Additionally, it must be noted that the interaction energies increase with increasing element number of the chalcogen atom X (i.e., O < S < Se < Te). In Figure 6a the potential energy profiles at the MP2/cc-pVTZ-ECP level of theory for the alkyne-containing model systems **2**, **5**, **8**, and **11** are shown. It can be seen (cf. Table 2) that the equilibrium distance increases only slightly between **2**, **5**, and **8**, but considerably for **11**. The interaction energy increases from 2.58 kcal/mol (**2**) to 4.64 kcal/mol (**11**). In Figure 6b we kept the chalcogen center constant (Se) and varied the substituents from CH_3 (**7**) via C_2H (**8**) to CN (**9**). This leads to a decrease in $r(X_1,X_2)$ and an increase in the interaction energy.

The calculated chalcogen−chalcogen vibrations of **1**−**12** are in the order of 20−50 cm^{-1} (see SI). The X_2-Z stretching mode was found to be the most influenced vibration by dimer formation. The corresponding changes in the vibrational frequencies $\Delta\tilde{\nu}(X_2-Z)$ are shown in Table 2. The frequency decreases within each family **4**−**6**, **7**−**9**, and **10**−**12**, but not in

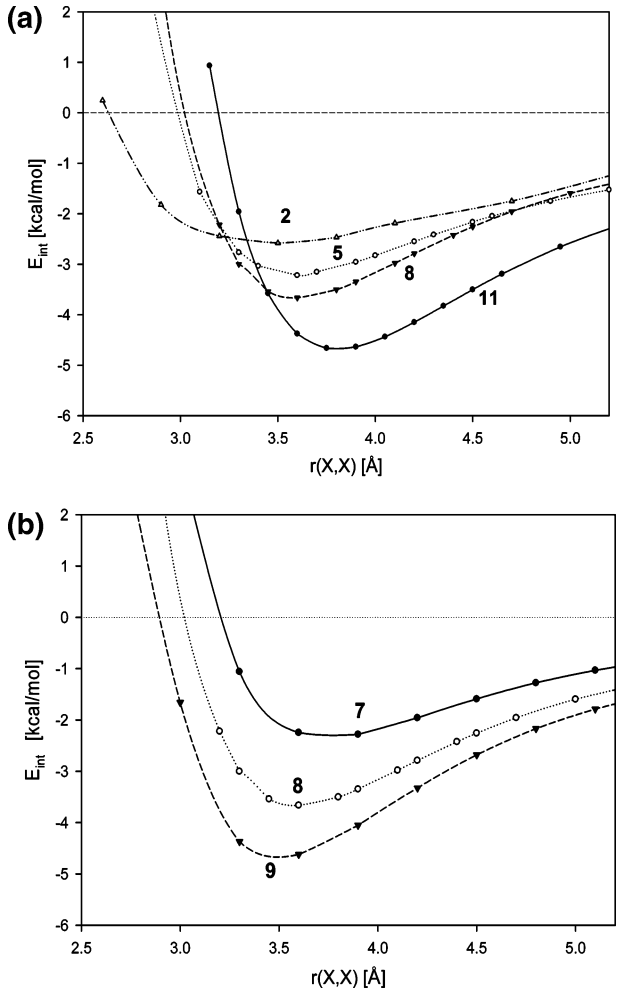

Figure 6. (a) Interaction energies of alkynyl substituted aggregates **2**, **5**, **8**, and **11** as a function of $r(X_1,X_2)$. (b) Interaction energies of selenium-containing aggregates **7**−**9** as a function of $r(X_1,X_2)$.

1−**3**. In the same manner, the decrease in vibrational frequency is accompanied by an increase in bond length of the X_2-Z bond (see SI). This observation can be rationalized by the results mentioned above, which predicted p−σ* type interactions to occur within the families **4**−**6**, **7**−**9**, and **10**−**12**, but not in **1**−**3**.

These trends summarized in Table 2 and visualized in Figure 6, a and b, are in qualitative agreement with the interaction model shown in Figure 2. According to this qualitative model the interaction should increase with decreasing energy difference between the p donor orbital and the $\sigma^*_{X_2-C}$ acceptor orbital. The energy of the acceptor orbital decreases in the series O → S → Se → Te and Me → C_2H → CN. The energy of the donor orbital increases in the series O → S → Se → Te as exemplified by the ionization energies of Me_2X (X = O, S, Se, Te).[47,48]

Symmetry Adapted Perturbation Theoretical (SAPT) Studies. In the computational details section it was noted that a highly correlated method is necessary to account for the specific nature of a noncovalent contact. As a consequence, the approximations used in the MO-SCF procedure resulted in significant deviations from electron-correlated results in lieu of structural (i.e. intermonomeric distance $r(X_1,X_2)$) as well as energetic criteria. However, in the previous paragraph we have successfully applied this one-electron picture for rationalizing the trends found by electron-correlated methods for the systems

Table 3. Partition of the Energies [kcal/mol] Derived from SAPT Calculations in Electrostatic (E_{elst}), Inductive (E_{ind}), Dispersive (E_{disp}), and Exchange (E_{exch}) Energies for Model Systems **1**−**9**, as Defined by eqs 3−6

model system	E_{elst}	E_{ind}	E_{disp}	E_{exch}	$E_{int,SAPT}^{6-311G^{**}}$ [a]
1	−0.12	−0.38	−1.85	0.72	−1.83
2	−0.56	−0.37	−1.82	0.52	−2.25
3	−0.97	−0.43	−1.71	0.74	−2.64
4	0.43	−0.32	−2.12	0.39	−1.92
5	0.72	−0.36	−2.41	0.52	−1.92
6	0.82	−0.53	−2.57	0.64	−2.21
7	0.90	−0.38	−2.86	0.54	−2.23
8	1.34	−0.68	−3.41	0.86	−2.56
9	1.62	−1.22	−3.75	1.07	−3.25

[a] The last column collects the sum of the four contributions plus δ_{HF}. For details see SI.

1−**12** regarding their geometrical arrangement as well as their interaction energy. Therefore, to address the nature of the noncovalent interaction between supermolecular aggregates such as **1**−**12**, we adopted the terminology derived from the symmetry adapted perturbation theoretic (SAPT)[43] treatment. In this approach the interaction energy E_{int} is calculated as an (infinite) expansion consisting of four principal components termed electrostatic (E_{elst}), induction (E_{ind}), dispersion (E_{disp}), and exchange (E_{exch}) energies (eq 2). For practical applications, each expansion coefficient $E^{(n)}_{SAPT}$ is approximated using a perturbation expansion from the Hartree−Fock wave function. In effect, this amounts to a double perturbation approach for the total interaction energy $E_{int,SAPT}$.

$$E_{int,SAPT} = \sum_{n=1}^{\infty} E^{(n)}_{SAPT} = \sum_{n=1}^{\infty}\sum_{k=0}^{\infty} E^{(nk)}_{SAPT} \qquad (2)$$

In practice, these infinite expansions are truncated after a finite number of terms, and in the presently available implementation (SAPT2002)[43] $E_{int,SAPT}$ is calculated as (for details see ref 43):

$$E_{int,SAPT} = E^{(10)}_{pol} + E^{(10)}_{exch} + E^{(20)}_{ind,resp} + E^{(20)}_{exch-ind,resp} + \delta_{HF} + \epsilon^{(1)}_{pol}(3) + \epsilon^{(1)}_{exch}(2) + E^{(20)}_{disp} + E^{(20)}_{disp} + \epsilon^{(2)}_{disp}(2) + E^{(20)}_{exch-disp}$$

To investigate the relative influence of the four principal forces, we have used eqs 3−6 to sum up several expansion coefficients resulting in a partition of E_{int} into E_{elst}, E_{ind}, E_{disp}, and E_{exch}. Although this partitioning scheme is not unambiguous, in the SI we provide a reasoning for it.

$$E_{elst} = E_{pol}{}^{(10)} + E_{exch}{}^{(10)} + \epsilon_{pol}{}^{(1)} \qquad (3)$$

$$E_{ind} = E^{(20)}_{ind,resp} + E^{(20)}_{exch-ind,resp} \qquad (4)$$

$$E_{disp} = E^{(20)}_{disp} + \epsilon^{(2)}_{disp}(2) + E^{(20)}_{exch-disp} \qquad (5)$$

$$E_{exch} = \epsilon_{exch}{}^{(1)}(2) \qquad (6)$$

The results of the SAPT calculations are summarized in Table 3 and are depicted in Figure 7. We note the dispersion force E_{disp} to be the major contribution in all systems **1**−**9**. The induction energy E_{ind} also is of a bonding type in all systems **1**−**9**, albeit to a much lesser extent. Despite these overall agreements, a clear-cut difference in the nature of the inter-

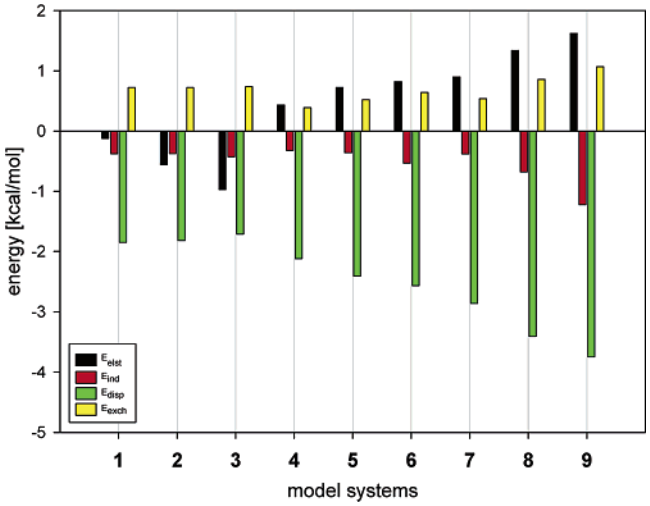

Figure 7. Contributions of the electrostatic (E_{elst}), induction (E_{ind}), dispersion (E_{disp}) and exchange correlation (E_{exch}) energies derived by the SAPT2002 program[43] and summed according to eqs 3−6.

molecular bond is observed between the oxygen-containing compounds **1**−**3** on one hand and the sulfur- or selenium-containing compounds **4**−**9** on the other. This simply reflects the observations made in the previous paragraph. For the latter cases, we note that the absolute value of both the dispersion and induction energy increases when changing the substituent Z from CH_3 via C_2H to CN. However, induction increases stronger rendering this more important for Z = CN than for Z = CH_3. This behavior is more clearly seen for Se than for S, reflecting the higher polarizability of Se. For the S- and Se-containing compounds, the electrostatic and exchange energies are antibonding. Due to the even higher polarizability of Te, these trends are expected to be even more evident for the tellurium-containing complexes **10**−**12**. We refrain from SAPT calculations of **10**−**12** due to the fact that only very small basis sets without ECP are available for tellurium.

These findings for the systems **4**−**9** are in strong contrast to the oxygen-containing aggregates **1**−**3**. Here, dispersion decreases slightly when going from Z = CH_3 via C_2H to CN, although it still remains the major bonding force. Induction energy is not affected by the substituent Z, reflecting the poor polarizability of oxygen. The greatest contrast is, however, the strongly bonding contribution of the electrostatic energy, which also shows great increase when changing Z from CH_3 via C_2H to CN.

These different behaviors of the oxygen-containing systems **1**−**3** on one hand and the compounds of the heavier elements S, Se, and Te on the other are seen throughout this work and can be rationalized by supposing that the principal interactions in the oxygen-containing compounds are (weak) hydrogen bonds, whereas in the other compounds interactions between the chalcogen atoms prevail. Considering the generally accepted notion,[16,17,49] that conventional hydrogen bonds are largely electrostatic in origin, we note **1**−**3** to represent an intermediate type between a classical hydrogen bond and a typical van der Waals force. This was noted previously[49] to be typical for C−H···Y type hydrogen bonds. The increase of E_{elst} in **1**−**3** is due to the increased dipole moment when changing Z from an electron-donating group (CH_3) to an electron-withdrawing group (CN). In the same line, E_{disp} is reduced due to a reduced polarizability of the acceptor oxygen. In contrast to compounds

Table 4. Partition of Interaction Terms for Model Systems **1**−**12** as Derived by a NBO Second-Order Perturbation Analysis in Chalcogen−Chalcogen Interactions (E_{X-X}) and Hydrogen Bonding (E_{H-bond})[a]

model system	E_{X-X}	E_{H-bond}	E_{max}	CT	model system	E_{X-X}	E_{H-bond}	E_{max}	CT
1	0.00	5.08	1.12	−3.86	**7**	2.41	2.83	0.76	+2.05
2	0.00	2.81	0.63	+1.80	**8**	4.42	1.75	2.13	+14.02
3	0.05	2.24	0.74	+5.31	**9**	7.17	1.48	3.97	+25.26
4	0.13	4.18	0.68	−1.35	**10**	5.99	2.45	3.43	+15.06
5	1.82	1.93	1.04	+5.41	**11**	10.85	1.78	7.30	+37.81
6	3.02	1.50	1.85	+11.78	**12**	17.50	1.44	12.68	+65.19

[a] The largest matrix element of the perturbation analysis is given as well (E_{max}). For **1**−**4** this amounts to hydrogen bonding, while for **5**−**12** it is of p−σ^* nature. All values are given in kcal/mol. The charge transfer (CT) from donating units ($(CH_3)_2X_1$) to accepting units ($(CH_3)_2X_2Z$) is given in 10^{-3} electrons.

1−**3**, which are dominated by hydrogen bonds, **4**−**12** show an increasingly dominating chalcogen−chalcogen bonding. This type of interaction is based on the (static as well as dynamic) polarizability of the chalcogen atoms (S, Se, Te) involved, resulting in the dominance of E_{disp} and E_{ind} in these aggregates. In conclusion, the SAPT calculations show an increasing influence of polarizability on the intermolecular attraction with increased atomic number of the chalcogens involved, whereas in the same line the electrostatic interaction becomes repulsive. A clear-cut difference is observed between O on one hand and S, Se, and Te on the other, suggesting that weak hydrogen bonds prevail in **1**−**3**, whereas chalcogen−chalcogen interactions become increasingly dominating in **4**−**12**.

NBO Analyses. As an alternative to the analysis given in the previous paragraph, a noncovalent interaction can be characterized in terms of the functional chemical groups involved. In our case, this amounts to hydrogen bonding between C−H groups and a chalcogen atom and to chalcogen−chalcogen interaction between the two chalcogen centers X_1 and X_2. In view of the experimental results described[12−16] in the Introduction, this subdivision is reasonable. To unravel the various contributions, we used NBO analysis. This was done for **1**−**12** by interpreting the sums of the second-order interaction terms of the NBO program in terms of hydrogen and chalcogen−chalcogen bonding (a detailed description of the summation algorithm is provided in the SI). The results of this study are summarized in Table 4. When interpreting the results, it should be considered that this approach is only performed at the HF-SCF level of theory (i.e. the Fock operator is analyzed in the basis of the NBOs), and that any interaction will only be bonding (i.e. antibonding contributions are not covered by an NBO analysis and must be calculated separately), rendering the results of this approach useful only for a qualitative discussion here. Nevertheless, we find this an elegant way to gain insight into the principal interacting functional groups. It is notable that the absolute values of hydrogen bonding are nearly constant for the aggregates **7**−**12** (only ranging from 1.4 to 2.8 kcal/mol) compared to those for the chalcogen−chalcogen interaction (ranging from 2.4 to 17.5 kcal/mol). In none of these compounds but **7** we find a hydrogen bond stronger than the chalcogen−chalcogen interaction. The variance as well as the absolute values of the hydrogen bonds for the sulfur-containing dimers **4**−**6** are somewhat larger (4.2 to 1.5 kcal/mol). Here, we observe a transition from a hydrogen-bonded complex (**4**) to a chalcogen−chalcogen-bonded complex (**6**). For systems **5**−**12** the major single intermolecular NBO interaction term is

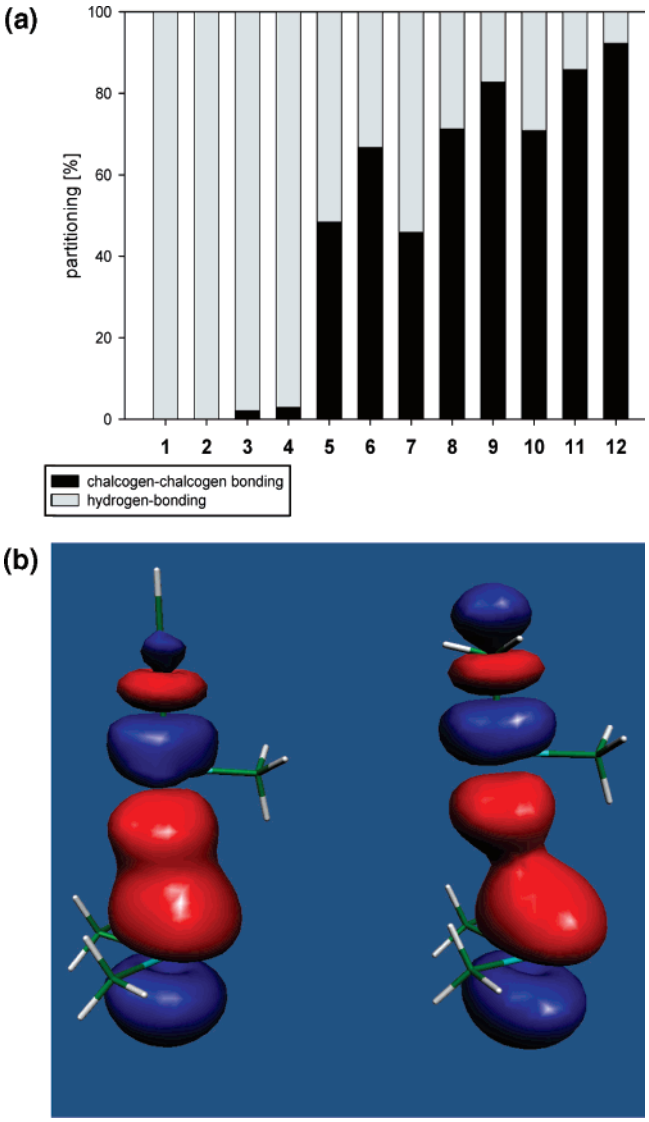

Figure 8. (a) Relative contributions of the hydrogen and chalcogen−chalcogen bonding as derived from NBO calculations. (b) Isosurfaces for a value of 0.04 showing the linear combinations of 5p of $Te(CH_3)_2$ and the σ^* orbital of $Te-CH_3$ (**10**, right) and $Te-C_2H$ (**11**, left).

of p−σ^* type. For the oxygen-containing dimers **1**−**3** the strongest variance of hydrogen bonds (5.1 to 2.2 kcal/mol) occurs, and basically no oxygen−oxygen interactions are found. Here, we also note an inconsistency between the trends of the overall interaction energy predicted by the NBO analysis and $E_{int,MP2}^{cc-pVTZ-ECP}$ (cf. Table 2) demonstrating the limits of this approach.

However, on a qualitative basis, these numbers strongly support the findings of the supermolecular and the SAPT calculations. The relative dominance of each contribution is more clearly visualized in Figure 8a, in which the two competing interactions (summed up to 100%) are plotted. We note a predominance of hydrogen bonds for the oxygen-containing systems **1**−**3**. This is in accordance with our assumptions described in the previous paragraph. For compounds **8**−**12** (Se and Te families) we report predominating chalcogen−chalcogen interactions—a fact that is also corroborated by the SAPT calculations and based on the high polarizability of Se and Te. The aggregates **4**−**7** (S family and the least bonded Se compound) represent transitions in which the hydrogen bond

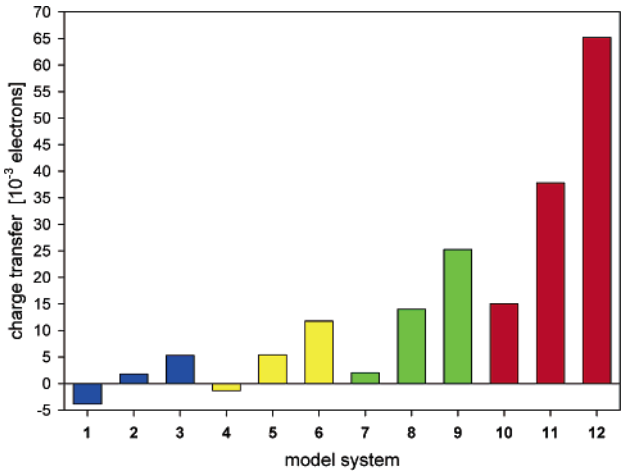

Figure 9. Charge transfer for the model systems **1**−**12** from the donating units ($(CH_3)_2X_1$) to the accepting units (CH_3X_2Z).

becomes less dominating and the interaction between the chalcogen centers becomes increasingly competitive. This observation is also reflected by the SAPT investigations where the electrostatic interaction becomes increasingly repulsive and dispersion becomes increasingly attractive, indicating some type of transition between prevailing hydrogen-bonded character with a strong electrostatic nature (such as in **1**−**3**) and chalcogen−chalcogen interaction character with a strong dispersive and inductive nature (such as in **8**−**12**).

These findings are supported by the charge transfer (CT) given in Table 4. We observe a steady increase in CT from one monomer to the other in each family, e.g. **1**−**3**, **4**−**6**, **7**−**9**, and **10**−**12** (see Figure 9) with a tendency toward a more distinct and positive CT. A negative value is attributed to a CT from CH_3-X_2-Z (Z = CH_3, C_2H, CN) to the monomer $(CH_3)_2X_1$ and is observed for systems **1** ($X_1 = X_2 = O$) and **4** ($X_1 = X_2 = S$). In these systems hydrogen bonding prevails, and we note two hydrogen bonds of $X_2\cdots H_3C-X_1$ in contrast to only one of $X_1\cdots H_3C-X_2$ (cf. Figure 5). Thus, a net CT from monomer CH_3X_2Z to $(CH_3)_2X_1$ results. Substituting for Z = CH_3, C_2H, and CN strengthens the $X_1\cdots CH_3-X_2$ hydrogen bond, but weakens the other two. As a result the CT values become more positive (Figure 9). For **4**−**6**, and analogously for **7**−**9** and **10**−**12**, we observe a steady increase in CT caused by significant p−σ^* interactions. An analogous trend is observed for chalcogen−chalcogen interactions.

The influence of the substituent Z is demonstrated in Figure 8b, showing the isosurface with a value of 0.04 for the bonding linear combinations between the 5p donor orbital of $Te(CH_3)_2$ and the σ^* orbital of the Te−Z bond (Z = CH_3, **10**, and Z = C_2H, **11**). A much stronger interaction between 5p and σ^* can be noticed for **11** than for **10**.

Concluding Remarks and Perspectives

In this paper we investigated intermolecular interactions between two molecules containing group VI elements. The strength of this interaction increases steadily when going from oxygen (**1**−**3**) via sulfur (**4**−**6**) to selenium (**7**−**9**) and reaches its maximum of about 6 kcal/mol for tellurium (**10**−**12**). In each of these families we observe an increased bonding when adding an electron-withdrawing substituent such as alkynyl or cyanide to the group VI element. Despite this clear trend, we definitely

observe a competition between weak hydrogen bonds of the C−H···Y kind and a novel type of interaction taking place solely between the group VI elements (termed here as chalcogen−chalcogen interactions). In those compounds containing hardly polarizable and highly electronegative oxygen atoms, so-called improper hydrogen bonds dominate the interaction and basically no chalcogen−chalcogen interactions are observed. However, with increasing polarizability of the group VI elements, the chalcogen−chalcogen type interaction strongly increases resulting in its overall domination in the tellurium-containing systems. The relative strength of the hydrogen bonds vis-à-vis the chalcogen−chalcogen interactions can be controlled by varying the substituents on the chalcogen atom for the intermediate cases sulfur and selenium. As frequently observed, the greatest change in type of interaction occurs when substituting oxygen by sulfur.

In considering the electronic properties of the intermolecular interaction, we note that dispersion represents the major bonding force in all systems **1**−**12**. However, a clear-cut difference between the oxygen-containing compounds **1**−**3** and the systems containing the heavier chalcogens **4**−**12** was observed, once again indicating the great change when going from a first period element to one of a higher period.

While for the oxygen-containing aggregates **1**−**3** the electrostatic effects were found to be bonding and relatively important, this is diametrically different for the dimers **4**−**12**. In the latter case induction forces are attractive, while the electrostatic contribution becomes repulsive. This tendency is more elaborately seen in the selenium aggregates than in the sulfur ones, reflecting the higher polarizability of selenium. A distinct difference within the families is also observed. For the oxygen-containing compounds, the electrostatic interaction becomes much more attractive when substituting oxygen with electron-withdrawing substituents, while dispersion and induction basically remain the same. This is different in **4**−**12**, where in each family the attractions due to induction and dispersion strongly increase, while electrostatic effects become more repulsive.

Our calculations show that electron-correlation is necessary for a quantitatively correct description of the chalcogen−chalcogen interaction. However, the one-electron p−σ* model (Figure 2) derived from HF-SCF calculations performs qualitatively well (see also Figure 3). For **4**−**12** the trend of the dispersion interaction is similar to that of the electrostatic and inductive forces. Because these are partly covered at the HF-SCF level of theory, we notice a correspondence between the trends calculated in the HF-SCF model and electron correlation methods resulting in a qualitative agreement between the one-electron picture (Figure 2) and that derived by the electron-correlated calculations. However, when interpreting experimental results or synthesizing new compounds the soundness of p−σ* interactions should not be overemphasized.

We explain our observations by the electronic properties of the respective group VI elements. With the increasing polarizability of the group VI elements when going from oxygen to tellurium, dispersion and inductive components become more important. Therefore, we see a steady increase of dispersion and induction when going from **1** via **4** to **7** (and analogously for **2**, **5**, **8** and **3**, **6**, **9**). In the same manner, the electrostatic interaction becomes more repulsive when going from oxygen to higher group VI elements.

These results show that a strong intermolecular interaction with a major electrostatic contribution can be anticipated from two hard components. The most well-known example is the conventional hydrogen bond between a hard hydrogen donor (O−H) and a hard hydrogen acceptor (O). The interaction between a soft hydrogen donor and a hard acceptor (O, S) will result in less stabilization as exemplified in systems **1**−**4**. For these hydrogen-bonded systems, we do not find a strong electrostatic or dispersion force. A strong interaction in which dispersion and induction forces dominate is expected from two soft components. This is the case in **8**−**12** and can easily be extended to other combinations such as compounds containing group V or group VII elements. This view is supported by the fact that in crystal engineering halogen−halogen,[11] chalcogen−chalcogen[13−15] interactions as well as the van der Waals bonding between halogen centers and other lone-pair-possessing atoms play a pivotal role.[50] Furthermore, our results show that also in intramolecular interactions between chalcogens and other lone-pair-possessing atoms[22,33] the improper hydrogen bonds cannot be neglected. The energy values listed in Table 2 suggest that experimental evidence for the existence of such pairs in the gas phase should be within reach by applying modern spectroscopic means, e.g. rotational spectroscopy or mass spectrometry.

Acknowledgment. This research was supported by the Deutsche Forschungsgemeinschaft (DFG) and the Fonds der Chemischen Industrie. D.B.W. is grateful to the Graduiertenkolleg 850 (Molecular Modelling) and to the Studienstiftung des deutschen Volkes for a graduate fellowship. We thank B. Esser and G. Jansen for helpful discussions and P. Krämer for typing the manuscript.

Supporting Information Available: Cartesian coordinates, absolute energies for the compounds **1**−**12**, details of the SAPT calculations; detailed description of the methods and basis set benchmark studies, a detailed description of SAPT and NBO summation algorithms; complete refs 40 and 43. This material is available free of charge via the Internet at http://pubs.acs.org.

JA056827G